RSC Sustainability

ROYAL SOCIETY OF CHEMISTRY

PAPER

View Article Online
View Journal | View Issue

Check for updates

Cite this: *RSC Sustainability*, 2025, **3**, 3060

Sustainable packaging solutions: harnessing primary sludge cellulosic fibres in foamed starch materials *via* injection moulding†

Susana C. Pinto, *[a] Bernardo Graça,[a] Vasco G. Lopes[b] and Dmitry. V. Evtuguin *[a]

Driven by stringent environmental regulations and keen social awareness, the pulp and paper industry is increasingly challenged by the growing volume of residues generated, highlighting the need for more comprehensive plants and to find solutions to transform biowastes into value-added products. Tackling this problem while replacing synthetic polymer packaging with natural alternatives is challenging, but it also provides an opportunity to address both issues. The main objective of this study was to develop sustainable packaging solutions using primary sludge, a major cellulose fibre residue from the paper industry. For the purpose, the sludges were combined with starch, a natural polymer, to produce foamed trays *via* injection moulding, using water as plasticizing and blowing agent. The injection moulding conditions were optimized, and the physical properties and microstructure of the resulting materials were evaluated. The results showed that foamed trays could be successfully produced using formulations with up to 28% wt of primary sludge incorporated into a starch matrix through injection moulding. The resulting trays had a cellular foamed structure with a dense hard hydrophobic surface layer, displaying a water contact angle greater than 115°. The foamed inner structure contributed for the low density of about 0.500 g cm^{-3} and the high-water absorption capacity. The packaging material revealed flexural stress values varying in the order of 5.0–7.0 MPa and flexural modulus of 370–450 MPa. This study demonstrated that sustainable 3D foamed packaging materials can be produced from natural and waste materials using injection moulding, representing a shift from earlier thermopressing methods traditionally used for manufacture starch-based biocomposites.

Received 20th February 2025
Accepted 26th May 2025

DOI: 10.1039/d5su00118h

rsc.li/rscsus

Open Access Article. Published on 03 June 2025. Downloaded on 2/14/2026 7:58:34 PM.
This article is licensed under a Creative Commons Attribution 3.0 Unported Licence.

Sustainability spotlight

In this work, primary sludge from the paper industry was combined with a natural polymer, starch, to produce 3D foamed trays using injection moulding. This approach not only contributes to circular economy practices by finding value-added applications for primary sludge but also fosters the development of eco-friendly products, reducing reliance on non-renewable resources. Additionally, the use of injection moulding enables efficient production with minimum waste, further supporting environmentally responsible manufacturing.

1 Introduction

The pulp and paper industry is of great strategic importance worldwide and constitutes one of the main sources of income for Portugal economy.[1] The production of solid waste by these industries remains high and is steadily increasing each year, estimated at an average of 23.4% sludge per unit of paper production.[2] A distinction is made between primary and secondary sludge. The most abundant primary sludge refers to the material generated by the clarification of initial raw paper/pulp mill effluent *via* sedimentation or flotation. This matter is rich in cellulosic fibres. Secondary sludge is the residue after biological treatment of clarified wastewater and consists mainly of bacterial flocs. The most common disposal procedures for sludges are in landfills. However, due to the increasing costs incurred by landfills and new legislation constantly being developed to reduce landfill waste, it is becoming increasingly challenging to find suitable solutions and comply with ever more stringent environmental requirements.[2,3] Therefore, from an environmental and socioeconomic point of view, it becomes urgent for the academic and industrial sectors to apply appropriate technologies and economically efficient processes to transform waste from the pulp and paper industries into high value-added products for the well-being of society.[2,4] So far, the applications of the sludge include energy production,[2,5]

[a]*CICECO-Aveiro Institute of Materials, Department of Chemistry, University of Aveiro, Aveiro, 3810-193, Portugal. E-mail: scpinto@ua.pt; dmitrye@ua.pt*

[b]*ThinkPack – Lab & Packaging Center, Lda, Bairro do Serrado – Edifício F Lote 6, 3500-092 Viseu, Portugal*

† Electronic supplementary information (ESI) available. See DOI: https://doi.org/10.1039/d5su00118h

© 2025 The Author(s). Published by the Royal Society of Chemistry

Open Access Article. Published on 03 June 2025. Downloaded on 2/14/2026 7:58:34 PM. This article is licensed under a Creative Commons Attribution 3.0 Unported Licence.

construction sector – application in bricks, light aggregates and cement production,[6] insulating materials[7] and environment applications, as sorbents.[8,9] Since the composition of pulp and paper mill primary sludge mainly consists of cellulosic fibres (short, long and debris), and inorganic residues (ash) they can be used as reinforcement fillers of many materials.[5] For example, due to high concentration of silica and magnesium salts found in paper primary sludge, they show great potential to be mixed with the cementitious material, presenting the advantage of increasing the setting time.[6]

At the same time, the tightening environmental regulations are driven researchers and industry to join forces in developing alternative polymers for packaging that are not derived from petroleum. In fact, addressing plastic pollution has emerged as a top priority for major global entities, including the United Nations (UN), the World Economic Forum (WEF), the World Health Organization (WHO), and the European Union (EU).[10,11] Government entities have established stringent guidelines targeting the significantly reducing the consumption of synthetic single-use plastics.[12,13] In this regard, the use of starch in the packaging industry as a substitute for the most common synthetic plastics is finding increasing application due to its availability, relatively low cost, biodegradability and excellent film-forming properties.[14]

Starch is a naturally occurring semi-crystalline polymer present in cereals (such as corn and wheat), tubers (potato, cassava), and leaves. It is constituted of water-sensitive granules, which size and morphology are influenced by its biological origin and ultimately determining the physicochemical properties of starch-based materials.[15] Native starch is not processable due to its granular structure and extensive hydrogen bonding. Under heat and shear forces, and in the presence of a plasticizing agent, native starch is transformed into thermoplastic starch (TPS), a processable material. TPS shares certain mechanical limitations with Polylactic acid (PLA) and cellulose-based materials, including low tensile strength and moisture sensitivity. Nevertheless, TPS offers key advantages for sustainable packaging applications, such as a faster degradation rate than PLA and lower processing temperatures compatible with conventional polymer processing equipment, enhancing both cost-efficiency and environmental performance.[12,13,16]

Blending starch with other polymers,[17] adding reinforcing materials to form composites,[18] crosslinking and coatings,[19] have been proposed to overcome starch limitations.[20] The most common processing techniques associated to starch-based packages are solvent casting, thermopressing and extrusion. Solvent casting is a simple and non-expensive method with no need for sophisticated machinery; however, its widely application is limited by the low capacity of production and the difficulty in expanding to an industrial scale. Thermocompression does not allow for complex geometries, the production time is high, and the automatization of the process is limited and generates wastes.[21] Single, twin – extrusion or co-extrusion needs to be combined to other techniques since the material comes out in the form of a die.[20] In extrusion process, the heating and shearing forces applied to the mixtures allow to the starch gelatinization. This system can be coupled to an injection moulding machine, for example. Injection moulding manufacturing technique allows producing a high number of 3D complex plastic designs with high degree of automation and at relative low costs.[22] In this process occurs a combination of pressure and high shear force conditions at the same time involving the complex thermomechanical dynamic behaviours of viscoelastic materials.[21,23] In the injection moulding, critical variables include material temperature, injection speed, mould temperature, and holding time. The material must be heated to the optimal temperature for proper flow and the injection speed must be regulated to avoid defects and ensure complete filling of the mould while the mould temperature must be maintained for effective solidification and cooling. Furthermore, holding time must be set appropriately to ensure the material fully fills the mould's shape and solidifies correctly. With the optimized formulation and processing conditions, manufacturers can achieve high-quality finishes, making the process both economically and time efficient. The optimization process makes injection moulding a competitive choice for producing intricate thermoplastic parts.[24]

In the packaging sector, foamed starch materials have advantages over the dense such as low density and cost-effectiveness.[14,25,26] Different techniques used for starch foaming have been developed, including extrusion foaming, baking/compression, solvent exchange/vacuum freeze-drying, and supercritical fluid CO_2-aid extrusion foaming to produce snacks in the food, loose fill chips for protective packaging and trays. So far, foamed starch-based packages, namely trays, have been produced mainly by hot thermopressing moulding.[26]

Regarding the numerous matrices that can be made by changing the formulation composition or injection moulding parameters, different properties can be obtained. Few information disclosures the utilization of starch-based materials by injection moulding[17] given the narrow range of viscosity of the mixture that worked for this process. It usually reports the blend of starch and other polymers, as examples: copolymer of ethylene and vinyl alcohol;[27] PLA and a blend of native tapioca starch and polyethylene.[28] Earlier studies reported the use of starch as main matrix enclosing fibres in percentages ranging from 0.5 to 20% wt and produced foamed pieces *via* thermopressing. Some examples are sugarcane bagasse fibres,[29] cellulose nanofibers from *Chrysopogon zizanioides* roots,[30] agro-industrial residues,[31] microcrystalline cellulose,[32] calcified green macroalga.[33] The incorporation of these type of cellulosic materials contributed to enhance the properties of the final products, as barrier properties, mechanical properties, *etc.* Also organically modified nanoclays[18] were incorporated in starch formulations.

This study aims to contribute with a practical solution for the valorisation of paper mill primary sludge by incorporating it into sustainable matrices, such as starch-based packaging, produced through injection moulding. The methodology consisted of five-stages: (i) characterization of primary sludges from Renova S.A. paper mill, (ii) preparation of the primary sludge and starch paste, (iii) fabrication of foamed trays from starch and sludge-based formulations *via* injection moulding –

Open Access Article. Published on 03 June 2025. Downloaded on 2/14/2026 7:58:34 PM. This article is licensed under a Creative Commons Attribution 3.0 Unported Licence.

injection parameters optimization (iv) selection of the foamed trays and (v) chemical, structural and mechanical characterization of selected foamed trays.

2 Materials and methodology

2.1. Materials

Industrial corn and potato starches were used. Primary fibre sludge from tissue paper production unit was provided by Renova S. A. (Torres Novas, Portugal) and kaolin powder was purchased from Mota Ceramics Solutions® (Oiã, Portugal).

2.2. Analyses

Primary fibre sludges were characterized regarding ashes and organic matter content. The determination of the ash content was carried out using a muffle at 500 °C following the ISO 1762.[34] The analysis of the dry matter content present in the primary sludge was carried out using an oven at 105 °C, according to the ISO 638.[35] The classification of the average of fibres according to their length and width, percentage of fines, short and long fibres and coarseness was determined *via* Lorentzen & Wettre L&W Fibre Tester. In these assays, 0.2 g of filtered fibres were analyzed, and 20 000 fibres were measured. An ICP-OES Jobin Yvon Activa M and an ICP-MS Thermo X Series were used to determine the concentration levels of heavy metals.

To withdraw fibres aggregates, which lead to non-homogeneous fibres distribution into the composites, the primary paper sludges were first dried at RT and milled to yield 0.5 mm sized particles and further analysed by scanning electron microscopy (SEM), Fourier transform infrared spectroscopy (FTIR-ATR) and X-ray diffraction (XRD).

The morphological features of corn and potato starches and milled primary paper sludge were examined by SEM using Hitachi TM4000 microscope (Japan) at an accelerating voltage of 15 kV. The powders were directly fixed on the aluminium support *via* double face carbon tape. The particle size was determined in a LS 13 320 Particle Size Analyzer. The crystallinity of starches and milled primary paper sludge was assessed by X-ray diffraction (XRD). The analysis was performed with a Panalytical diffractometer (Netherlands) using copper Kα radiation ($\lambda = 1.5418$ Å) under the operational conditions of 45 kV and 40 mA. All assays were performed with a ramp rate of 2° min^{-1}. The FTIR-ATR spectra were recorded using a Spectrum BX (PerkinElmer, Massachusetts, USA), mode from 4000 to 500 cm^{-1} at a resolution of 4 cm^{-1} and 64 scans.

The injection moulding assays were carried out using a tailor-made extruder coupled with a closing heating mould system (Fig. S1 in ESI†) on the installations of ThinkPack® enterprise (Portugal). The moulding system was kept at 155 °C. The mould zone had a liquid refrigeration system to accelerate the cooling of the trays. Following the appropriate holding and cooling times, the moulded pieces were extracted and stored for 7 days at 25 °C and 50% relative humidity before characterization.

The wettability of trays surface was evaluated by assessing the angle formed between a 3 μL water drop (sessile drop) and the material surface using Young–Laplace equation fitting method. The contact angle measurements were carried out in OCA Dataphysics equipment (Data Physics Corp., San Jose, CA). The water absorption capacity was performed using 30 × 10 mm samples. The samples were weighed dried and after soaked in distilled water for 6 and 24 h (the excess water was removed with tissue paper before measurements). The amount of absorbed water was calculated as the weight difference and expressed as the mass of the absorbed water per mass of the original sample. The reported values are the mean values of 3 different measurements. The increase in thickness was also determined by measuring the thickness before and after immersion in water. The water vapour transmission rate (WVTR) and water vapour permeability (WVP) values were evaluated at 23 °C and 50% relative humidity following ASTM E96/E96M[36] – desiccant method with minor modifications. The results correspond to the average of three measurements. Three-point bending flexural tests were conducted on 70 mm × 10 mm specimens in a Shimadzu AG-25TA (Japan) equipped with a cell load of 1 kN. The assays were performed at a speed rate of 10 mm min^{-1} and the initial support distance was set on 5 cm. Dynamic mechanical thermal analysis (DMA) was carried out using a Tritec 2000 equipment (Triton Technologies) in single cantilever bending mode. The testing temperature ranged from −50 to 150 °C at a constant test frequency of 1 Hz and heating rate of 2 °C min^{-1}. The values of storage modulus (E'), loss modulus (E''), and damping factor ($\tan\delta$) were recorded.

The thermal behaviour of the specimens was assessed by a SETSYS Evolution 1750 thermogravimetric analyser (Setaram, Caluire) at a scanning rate of 10 °C min^{-1} in the temperature range of 30–800 °C under synthetic air atmosphere (200 mL min^{-1}). Dynamic scanning calorimetry measurements were performed with a PerkinElmer Diamond DSC (Massachusetts, USA) differential scanning calorimeter equipment. All the measurements were performed in the temperature range of 30 to 250 °C at a heating rate of 10 °C min^{-1}.

The density and mechanical tests results were evaluated statistically in order to determine what or which ones were significantly different using one-way ANOVA and Tukey's *post hoc* tests at a significance level of 5%.

3 Results and discussion

3.1. Characterization of the primary sludge and starch

Table 1 gathers the information regarding the paper mill primary sludge characterization. Analysis of the sludge indicated a dry matter content of 23% wt comprising 22.7% wt of ash and 77.3% wt of organic matter (fines and fibres). Fines are small fibre's debris and any impurities representing 89.7% wt of the organic matter. The remaining 10.3% wt are classified as fibres, although with a small weight-average length (L_w). The fibres possessed an average width of 16.0 μm and a coarseness of 17.98 μg m^{-1}. The high percentage of fines in the primary sludge can be explained by the large number of damaged

© 2025 The Author(s). Published by the Royal Society of Chemistry

Open Access Article. Published on 03 June 2025. Downloaded on 2/14/2026 7:58:34 PM. This article is licensed under a Creative Commons Attribution 3.0 Unported Licence.

Table 1 General composition of the primary sludge

Ash content (% wt)	Organic matter (% wt)	Fines (<0.2 mm) (% wt)	Fibres (>0.2 mm) (% wt)	Fibre width (μm)	Length, L_w (mm)	Coarseness (μg m^{-1})
22.7 ± 2.4	77.3 ± 2.4	89.7 ± 3.9	10.3 ± 3.9	16.0 ± 0.6	0.17 ± 0.03	17.98 ± 1.62

recycled fibres, which easily pass through the forming wire of a paper machine and ends up in the wastewater. Longer fibres can become entangled with each other and form lumps, substantially increasing the viscosity of the starch-slurry mixture and making the injection moulding process more difficult. On the other hand, it is expected that the large number of fines could be easier incorporated into the starch-based mixture, having minor contribution to the increase in viscosity of the mixture and be easily processed.[37]

Regarding the composition of the ashes, the highest contribution was from Ca, Si, Al, Fe and Ti (Table S1 in ESI†). The content of such regulated transition metals as Cu, Zn and Mn was relatively low (below 30 ppm). The prevalence of Ca, Si, and Al in ash is due to the presence of respective inorganic fillers ($CaCO_3$, SiO_2 and kaolin) in the recycled papers used for the tissue paper production. Therefore, it is no coincidence that most of the calcium in primary sludge from a paper mill is in the carbonate form.[38] Due to the high ash content in the primary sludge (Table 1), this inorganic counterpart may affect negatively the preparation of the formulation with starch and the mechanical strength of the final composite after thermo-curing. This applies in particular to water-insoluble SiO_2 and kaolin, which can hinder the interfacial contact between fibres and between fibres and starch.

Regarding the starches under study, these revealed quite different granule's morphology (Fig. S2a and b in ESI†), which is commonly relates to the source of starches.[39] Thus, potato starch showed large round shaped granules ranging from 5 to 100 μm (d_L = 39.1 μm) of diameter and specific surface area of 0.138 m^2 g^{-1} (Table S2 in ESI†). On the other hand, corn starch granules were polyhedral with narrower size distribution from to 5 to 60 μm (d_L = 20.7 mm) and specific surface area of 0.259 m^2 g^{-1}. The starch granules have a diameter one order of magnitude smaller than the sludge flocs being fractionated (500 μm sieve) by hammer milling disintegration of the initial primary sludge (Fig. S2c in ESI†). More detailed structural information is provided below following the characterization of the obtained composites.

3.2. Production and characterization of packaging composites

3.2.1. Preparation of the formulation. The foamed packaging composites were prepared by injection moulding, from a formulation composed of 72% wt starch (50% wt corn starch and 22% wt potato starch), 28% wt primary sludge and 3% wt kaolin. This formulation was preselected according to a preliminary optimization study (details not presented or published).

The appropriate amounts of corn and potato starches, disintegrated primary sludge, and kaolin were mixed using a laboratory baking machine for 15 minutes at 50 °C. Subsequently, 50% wt of water (relative to the total mass of solids and water) was added, and the temperature was raised to 60 °C, with continuous mixing for an additional 20 minutes.

3.2.2. Production of packaging composites. The mixture was loaded into the hopper (Fig. S1 in ESI†) and conveyed through a screw rotating at 100 rpm with four heating zones (maintained at 60 °C) facilitating the plasticization and flow of the mixture. The general scheme regarding the methodology is shown in Fig. 1 and the injection parameters are summarized in Table 2. It is important to note that since the primary sludge was collected from the paper mill device that produced black tissue paper (toilet paper, napkins, *etc.*), the colour of this residue was also deeply dark. The resulting packaging prototype was a low-profile tray with rounded sides and thin walls (*ca.* 2 mm thickness) as shown in Fig. 1.

When submitted to different pressures and temperatures (as it occurs in the injection moulding process), polymers experienced physical phenomenon of thermal expansion and contraction, and its specific volume changes. Furthermore, the rapid transition between hot and cooling that occurs during injection moulding process can cause defects such as warpage, sink marks, and uneven shrinkage.[40–42] Accordingly, the basic parameters such as injected volume at certain injection rate and the total holding and cooling time were varied in order to obtain packaging prototype of acceptable quality (Table 2). To narrow down the number of samples and volume of work in characterization, a systematic selection methodology based on visual observations was applied. For the purpose, four parameters,

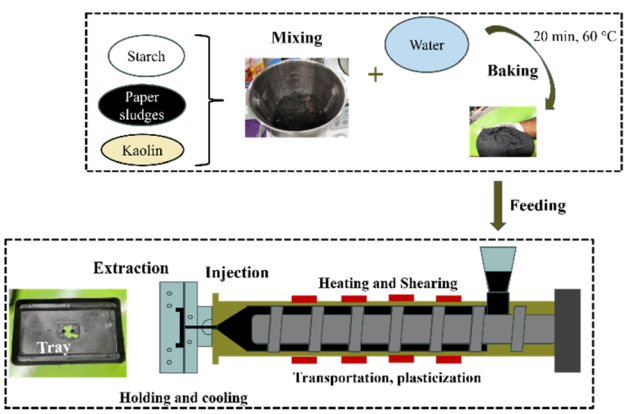

Fig. 1 Scheme of injection moulding process from the dough kneading (upper picture) to the tray extraction (lower picture) after compression moulding at 155 °C.

Open Access Article. Published on 03 June 2025. Downloaded on 2/14/2026 7:58:34 PM. This article is licensed under a Creative Commons Attribution 3.0 Unported Licence.

Table 2 Injection moulding conditions

Trays	Volume injected (cm^3)	Injection rate ($cm^3\ s^{-1}$)	Total time (s) (holding + cooling)
1	50	3	30 + 90
2	50	3	30 + 70
3	50	3	30 + 70
4	60	3	30 + 65
5	60	5	30 + 70
6	58	5	30 + 80
7	58	10	15 + 80
8	58	8	20 + 80
9	58	5	20 + 70
10	57	5	20 + 100
11	56	4	20 + 80
12	56	4	20 + 70
13	56	3	20 + 70
14	56	3	20 + 60
15	58	5	30 + 80
16	58	5	40 + 70

completeness of mould filling, pack uniformity, warpage, and finishing were set to select the conditions allowing to obtain the trays free defects or with less defects. If the trays fulfilled the criteria, it was attributed the classification of "+", otherwise "−". Based on the number of "+" attributed, the samples were categorized as poor (zero "+"); unsatisfactory (one +); satisfactory (two +), good (three +) and excellent (four +).

The results are gathered in Table 3. Trays 6, 11, 13 and 14 were chosen to further characterization since they have at least one distinct injection parameter and received at least the classification of "good" in the quality assessment.

3.2.3. Characterization of packaging composites

3.2.3.1. Infra-red spectroscopy. The FTIR spectra of the raw materials and tray 13 (only one tray spectrum is shown since the formulation is the same) are presented in Fig. 2a. The wide band located between 3600 and 3200 cm^{-1} corresponds to the stretching of hydroxyl groups present in the starches, cellulosic fibres from primary sludge and kaolin hydroxyl groups. The band at 1643 cm^{-1} corresponds to the bending of the water molecule that varies in intensity as a function of the amount of water that remains associated with the starch, sludge and kaolin. Small bands between 1500 and 1250 cm^{-1} can also be related to the local symmetry, such as CH_2 and the C–OH deformations in carbohydrates.[18,43,44] The characteristic IR absorption regions of starch (fingertip) are located between 1200 and 800 cm^{-1}.[45] The bands at 1150 cm^{-1} and 1078 cm^{-1} are associated with the stretching and the axial deformation of C–O–C bonds (glycosidic linkage) and C–OH, respectively. Bands positioned at approximately 1000 cm^{-1} have been identified as sensitive to the presence of water and related to the intramolecular hydrogen bonds of hydroxyl groups. The bands at 930 cm^{-1} correspond to C–H deformations of anomeric carbon α glucose in addition to being attributed to glycosidic bonds.[46,47] FTIR spectra of the paper primary sludge is similar to the starch spectra since sludge is composed of 80% wt fibres containing cellulose and hemicellulose. Regarding FTIR-ATR analysis, the spectrum of tray 13 contains both starches and paper primary sludges relevant bands with no appearance of new ones, suggesting that no additional bonds were formed. A small shoulder at the 668 cm^{-1} consistent with a peak in the paper primary sludge spectrum and kaolin spectra is absent in the starch one. This peak is not typical of polysaccharides, and therefore it can be concluded that it belongs to the metal oxides present in the primary sludge, *e.g.* iron oxide and magnesium oxide or silicates from kaolin. Tray 13 spectrum also presents a more intense peak at 1016 cm^{-1} comparatively to starch spectra commonly referred in literature as sensitive to the amorphous region of starch, while the band at 997 cm^{-1} is associated with the single helix crystalline structure.[44,47] As a result of the plasticization (water, shear forces and temperature) during the extrusion process, intramolecular and intermolecular hydrogen bonds between the hydroxyl groups in the starch chains are broken. The frequency shifts and intensity of the OH stretching was not significantly affected in the trays by adding the primary sludge, suggesting that the hydrogen-bond interaction of starch with a cellulosic material was weaker than that of starch molecule chains.[48]

Table 3 Quality assessment of composite trays based on visual analysis

Trays	Filling the mould	Uniformity	Warpage	Finishing	Classification
1	+	+	+	−	Good
2	−	−	−	−	Poor
3	−	−	−	−	Poor
4	+	+	−	−	Satisfactory
5	−	−	−	−	Poor
6	**+**	**+**	**−**	**+**	**Good**
7	+	+	−	+	Good
8	+	−	−	+	Satisfactory
9	+	−	−	+	Satisfactory
10	+	+	+	−	Good
11	**+**	**+**	**+**	**−**	**Good**
12	n.d.	n.d.	n.d.	n.d.	n.d.
13	**+**	**+**	**+**	**+**	**Excellent**
14	**+**	**−**	**+**	**+**	**Good**
15	+	+	−	+	Good
16	+	−	−	−	Unsatisfactory

3.2.3.2. X-ray diffraction. The XRD spectra of starch and primary paper sludge were shown in Fig. 2b. The potato and corn starches have a semicrystalline structure confirmed by the peaks obtained in XRD spectra. While corn starch presents A-type crystallinity with peaks at 15.3° and 23.1°, potato starch shows a pattern characteristic for B-type of crystallinity, which is represented by the peak at 17° (not observed for corn starch). A-type crystallinity indicates a structure with higher packing level while B-type structures are not so closely packed and the cavity between helical structures are filled with water molecules. These results agree with the patterns described in literature for these types of starches.[49] The XRD pattern of sludge showed peaks at 2θ 17.5, 20.2 and 24.8, suggesting the presence of calcite ($CaCO_3$), often used in paper production as filler and consistent with the metal analysis that identified the presence of calcium.[2,6] Tray's starch crystallinity is lower than that of

© 2025 The Author(s). Published by the Royal Society of Chemistry

Open Access Article. Published on 03 June 2025. Downloaded on 2/14/2026 7:58:34 PM.
This article is licensed under a Creative Commons Attribution 3.0 Unported Licence.

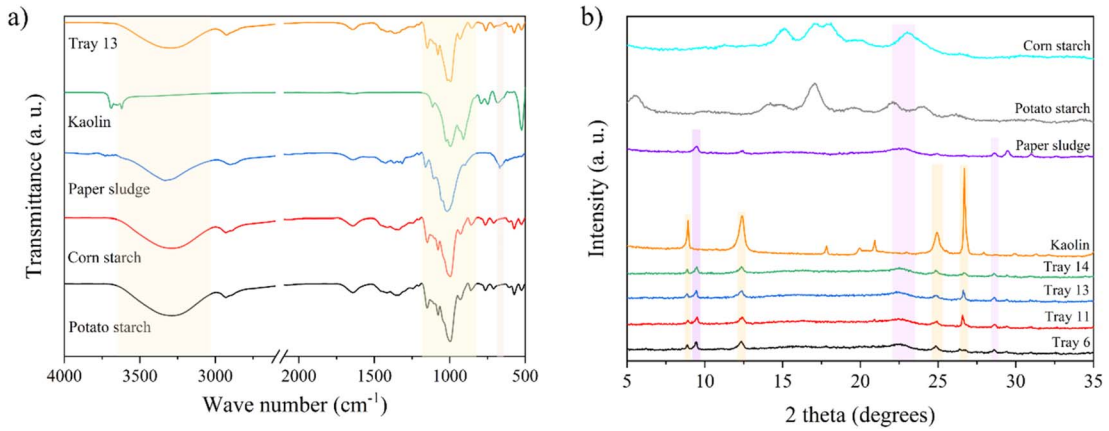

Fig. 2 (a) FTIR-ATR spectra of individual formulation components and obtained tray, and (b) XRD patterns of the initial raw materials and trays prototype samples produced thereof.

native starches. After the starch mixture is processed in porous trays through injection moulding, the XRD curve profile endures changes with the disappearance of the most of starch characteristic peaks as a result the paste undergo a high energetic process.[50] This is because natural crystals disappeared in the injection moulding process, with only a small number of residual crystals formed. This is consistent with FTIR-ATR analysis, where the intensity of the peaks corresponding to crystallinity phase decreased. The 2θ at 20° and 7° present in trays spectra are also observed in kaolin spectra. A small new peak located at 29° appear in trays patterns indicating a Vh-type crystallinity[32,51] due to the crystallinity of the starch chains forming a single helix structure combined with water and to the interactions of starch with the sludge components.[32,51]

3.2.3.3. Microstructure. Fig. 3 displays SEM micrographs illustrating cross-sections and the surfaces of the composite trays. These packaging composites exhibit a sandwich-type structure featuring a hard outer skin and a porous interior with cells showing a wide pore size distribution. Similar starch foamed structures were obtained by thermopressing using a bicomponent system of water and glycerol plasticizers.[26,29] In this study we were able to prepare porous structure using only water by injection moulding. Primary sludge particles were uniformly distributed within the walls of the inner cells (red arrows in the higher magnification images). During the preparation of starch-based formulation, water acted both as plasticizer and blowing agent, meaning that the water is used to gelatinize starch providing melt strength and enabling the expansion of the starch-based materials and part of water when heated above boiling point becomes gaseous and originates bubbles (blowing) essential to form the foamed structures.[52] The high temperature of the mould, 155 °C, leads to the formation of a dense layer conforming to the mould geometry. The mechanisms behind the formation of the cellular structure displayed in Fig. 3, with small pores near the surface and bigger pores in the core are related with temperature and pressure transfer mechanisms. When the mixture is forced to enter in the pre-heated mould, the temperature and pressure next to the surface are higher and therefore, the pores distribution is not uniform, with the formation of a thin layer of small pores next to the outer surface and big pores in the inside because of the escape of moisture and gases from the interior to the outside.

The phenomena of hornification can also occur because of the drying process taking place in injection moulding, which involve the removal of water from the cellulosic fibres resulting their surface collapse thus forming a hard surface.[53] The loss of water enhances the hydrogen bonds between cellulose fibrils, contributing to their rigidity and a loss of flexibility. Speculating on chemical similarities between starch and cellulose, one can propose their joint involvement in the hornification of the tray surface.

3.2.3.4. Wettability, water absorption capacity and water vapour transmission. The surface wettability or hydrophilic/hydrophobic nature of trays packages were evaluated through the water contact angle (WCA) measurement which was carried out by sessile drop methodology. All the WCA measurements were carried on the inner surface of the trays packages, which results are summarized in Fig. 4a. Surprisingly, all WCA values were higher than 115°, and therefore, the surfaces of the trays can be considered as hydrophobic ($\theta > 90°$). The water droplets did not spread and only slight reduction in contact angles values over time (at least for 3 min) were registered, probably due to the surface capillarity, thus suggesting minor interaction between water and the surface. SEM images (Fig. 3) show a hard surface with no or low porosity which means that the chemical composition is the major contributor for these high WCA values. This may be due to the hydrophobic extractables of the sludge and the hornification phenomena that occur between the cellulosic fibers and the starch under high processing temperature, which contributed to a low wettability of the composite material obtained. Inorganic fillers (*e.g.*, kaolin and silica) can also contribute to the surface hydrophobicity being interacting with accessible hydroxyl groups.[54] This proposition is corroborated by SEM-EDX analysis (Table S3 in ESI†) which indicates the presence of Si and Al belonging to primary sludge and kaolin, at the surface of the composite trays. This decrease in surface wettability in thermoplastic composites of starch/cellulose and cellulosic nanofibers/montmorillonite was also

Open Access Article. Published on 03 June 2025. Downloaded on 2/14/2026 7:58:34 PM.
This article is licensed under a Creative Commons Attribution 3.0 Unported Licence.

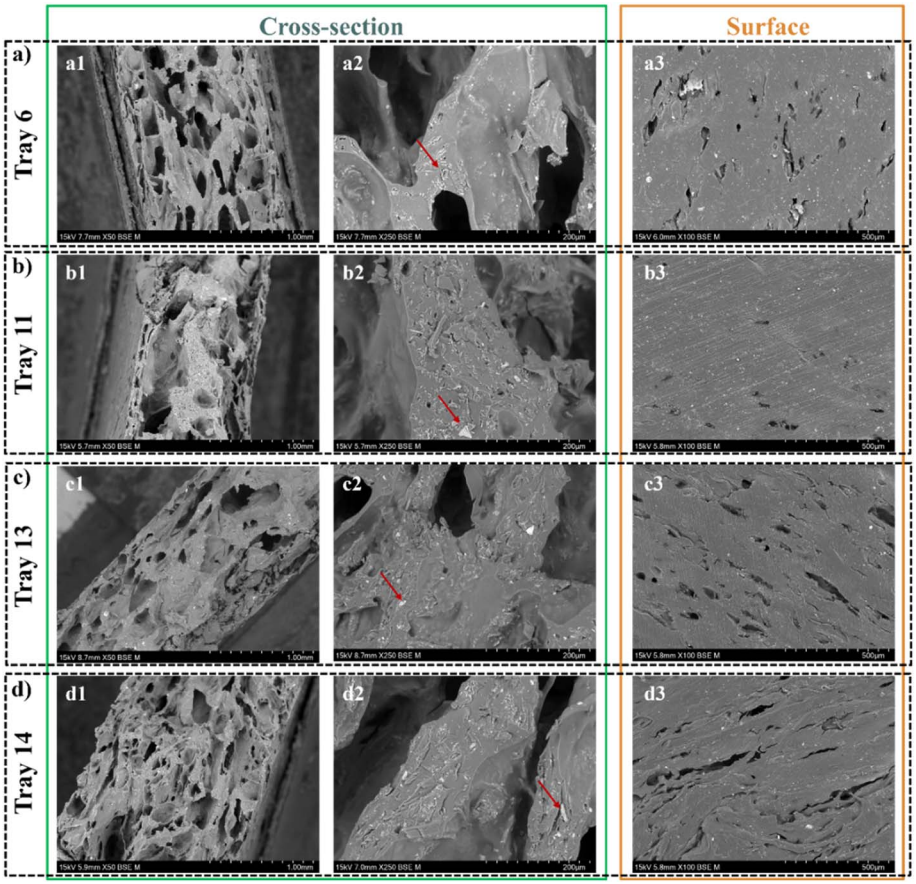

Fig. 3 SEM images of: (a) tray 6—(a1) cross-section, (a2) cross-section at higher magnification, and (a3) surface; (b) tray 11—(b1) cross-section, (b2) cross-section at higher magnification, and (b3) surface; (c) tray 13—(c1) cross-section, (c2) cross-section at higher magnification, and (c3) surface; and (d) tray 14—(d1) cross-section, (d2) cross-section at higher magnification, and (d3) surface.

observed by other researchers.[55] However, as was reported by Hassan *et al.*[56] for starch-microfibrillated cellulose boards produced by compression moulding, the addition of vegetable wax and poly(dimethylsiloxane)-based crosslinker was necessary to achieve the required hydrophobic properties of the composite material. The hydrophobic surface exhibited by the foamed composites obtained in this study is very interesting, since the commonly high surface hydrophilicity that characterizes starch-based products has limited applicability.

Regarding water absorption capacity Fig. 4b, when cutting the test specimens for analysis, the porous and hydrophilic internal structure allowed easy penetration and diffusion of water in the thin material, thus promoting its swelling. Following a 6 hour immersion, the specimens absorbed water

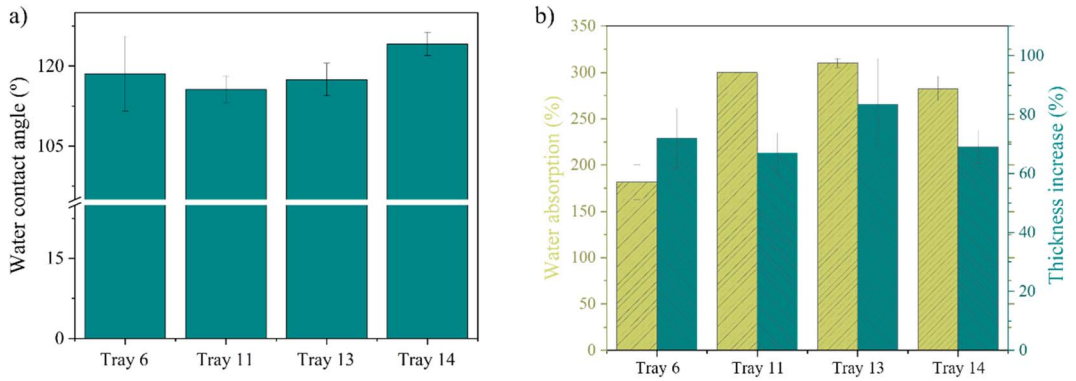

Fig. 4 (a) Water contact angle values and (b) water absorption capacity after 6 h of trays submerging in water and the respective increase in thickness.

© 2025 The Author(s). Published by the Royal Society of Chemistry

Open Access Article. Published on 03 June 2025. Downloaded on 2/14/2026 7:58:34 PM. This article is licensed under a Creative Commons Attribution 3.0 Unported Licence.

in the range of 180 to 310% (wt), leading to an approximate 1.6–2.0-fold increase in thickness. After 24 hours of immersion, the specimens lost their integrity, becoming difficult to handle and no measurements were done. Water molecules interact with starch hydroxyl free groups occurring disruption of starch–starch hydrogen bonding.[39] Cruz-Tirado *et al.*[39] correlated the substantial (55–90%) and rapid (within 1 minute) water absorption observed in starch-based trays with their porous structure and a significant number of accessible hydroxyl groups. The hydroxyl groups (confirmed by FTIR-ATR, Fig. 2a) could interacted readily with water molecules through hydrogen bonding. Tray 6 showed the lowest water absorption and thickness increase values. It is worth to mention that the ability to rapidly decompose in water, as observed for those trays, is one of the necessary conditions for quick biodegradation. The values of WVTR of 448 ± 9 g per m^2 per day and WVP of 21.3 ± 1.0 (g mm) $(m^2\ h\ kPa)^{-1}$ for tray 13 were in the same range of the 20–30 (g mm) $(m^2\ h\ kPa)^{-1}$ value, observed for 3 mm thick PLA trays containing carvacrol and cinnamaldehyde as natural antimicrobial essential oils, prepared by cast sheet extrusion and thermoforming.[57]

3.2.3.5. Density and flexural properties. The foam density of all trays ranged from 0.487 to 0.537 g cm^{-3} (Table 4) and is comparable to that reported in literature for starch-based foamed trays prepared by hot-pressing. Salgado *et al.* obtained trays with density varying between 0.456 to 0.587 g cm^{-3} for foams made of cassava starch, cellulose fibres, and sunflower protein isolate.[58] The ability of the trays packages to withstand bending deflection when an external force is applied was assessed by the flexural assays. It is reported in the literature that due to their semicrystalline structure and strong intermolecular bonding starch-based products are very rigid.[14] The use of water as the sole plasticizer has the dual effect of increasing cost-effectiveness and facilitating the creation of a highly porous structure. However, it also leads to the production of products with reduced flexibility, reflected by low deformation values (around 1.7–2.1%), Table 4. The trays exhibit flexural stress at break point values in the range of 5.01 to 6.98 MPa and flexural modulus between 370 and 447 MPa. Despite the slight adjustments made to the injection rate and cooling time parameters, it is anticipated only minor variations in the mechanical properties. However, a higher injection rate is expected to enhance chain orientation, decrease mobility, and consequently lead to stiffer materials. This phenomenon is observed when comparing trays packages 11, 13 and 14. A longer cooling time before opening the mould allows for more time for chain realignment.[59]

A higher injection rate (5 $cm^3\ s^{-1}$) and an extended formation time (30 s waiting time and 80 s with cooling) results in less rigid trays packages, as observed for tray 6 (Table 3). An example stress–strain curve for each tray package is presented in Fig. S3.† All tested specimens showed an initial short linear-elastic region until approximately 1% of deformation, followed by a rapid elastic–plastic behaviour reaching the maximum stress peak and after a sudden drop corresponding to failure. These results were comparable to those obtained by Moo-Tun *et al.*[27] with the advantage of using a simpler and with lower components system. The authors observed maximum stress values ranging from 1.5 to 2.7 MPa, and flexural modulus values varied between 160 and 210 MPa for packaging with different proportions of starch, PLA, cellulose, and $CaCO_3$ and using glycerol and water as plasticizers *via* thermoforming.[27]

3.2.3.6. Thermal properties. Fig. 5a presents the thermogravimetric analysis of tray 13, showing the weight loss as a function of temperature and the respective thermogravimetric derivate profile. Three stages of weight loss were detected. The first occurred between 50 and 150 °C and is related with the release of adsorbed water. This is consistent with the moisture content (10% wt, at 23 °C and RH of 50%). The second step occurred between 250 and 350 °C and represents almost 55% of weight loss. This stage involves the degradation of amylopectin and cellulose chains and subsequent degradation of monosaccharides with the release of volatile products. The maximum thermal degradation rate occurred at 304 °C. The final weight loss, occurring at temperatures as high as 380 °C and accounting for 15% weight loss is associated with the char formation.[39,60] At 450 °C, the char structural densification takes place, and the reorganization and diffusion of hydroxyl groups within the kaolin layer. Further slight mass at >600 °C loss is related to carbonate decomposition in carbon dioxide.[61] The residue at 800 °C is about of 22% wt composed primarily of ash, degradation products, and inorganic material. The DSC patterns of various tray samples are presented in Fig. 5b. The curves exhibit a similar trend, characterized by a gradual endothermic deviation as the temperature nears 100 °C, attributed to moisture evaporation. The exothermic deviation of DSC curve at T > 220 °C indicates the onset of thermal decomposition of both starch and cellulose. Previous studies have indicated that the glass transition temperature (T_g) of processed starch materials is detectable only when the heating

Table 4 Flexural mechanical properties of the trays 6, 11, 13 and 14. In each column, different letters indicate statistically different values (p < 0.05), using $n = 7$ for density and $n = 5$ for mechanical properties

	Density (g cm^{-3})	Flexural stress at break (MPa)	Deformation at break (%)	Flexural modulus (MPa)
Tray 6	$0.492 \pm 0.025^{a,b}$	5.01 ± 0.97^{a}	1.67 ± 0.10^{a}	370 ± 49^{a}
Tray 11	0.508 ± 0.015^{a}	6.98 ± 0.48^{b}	1.92 ± 0.19^{a}	447 ± 30^{b}
Tray 13	0.537 ± 0.014^{a}	6.57 ± 0.76^{b}	2.04 ± 0.39^{a}	$443 \pm 41^{a,b}$
Tray 14	0.487 ± 0.020^{b}	$5.98 \pm 0.65^{a,b}$	1.72 ± 0.28^{a}	$428 \pm 37^{a,b}$

© 2025 The Author(s). Published by the Royal Society of Chemistry

Open Access Article. Published on 03 June 2025. Downloaded on 2/14/2026 7:58:34 PM.
This article is licensed under a Creative Commons Attribution 3.0 Unported Licence.

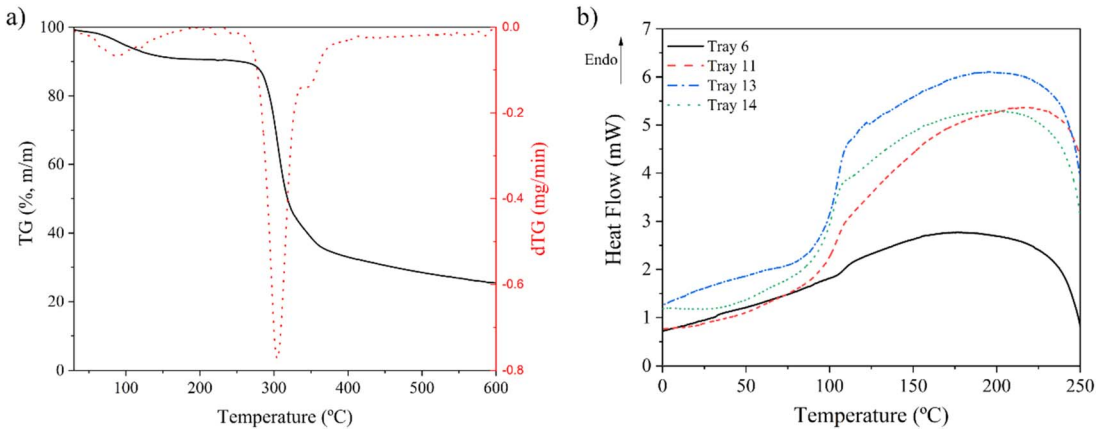

Fig. 5 (a) TGA and DTG curves of tray 13 under inert atmosphere (N_2) and (b) DSC patterns of the trays 6, 11, 13 and 14.

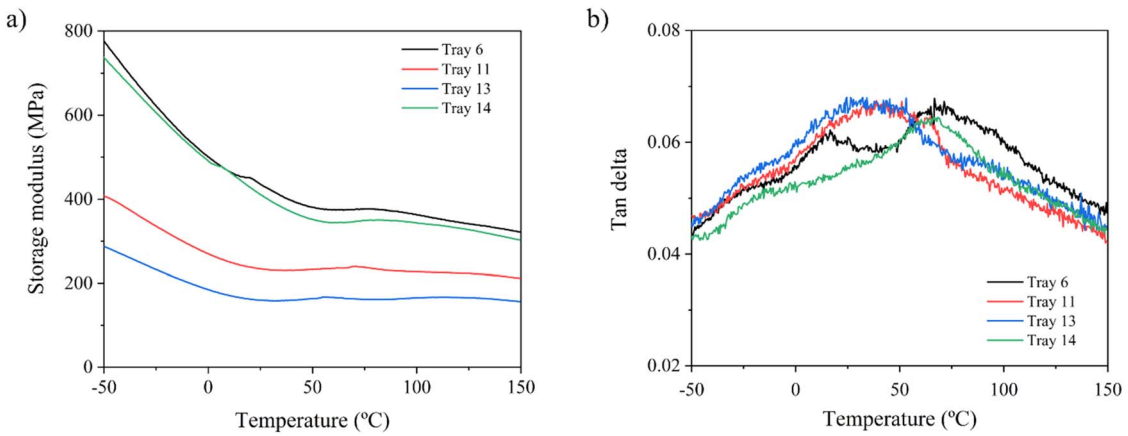

Fig. 6 (a) Storage modulus and (b) tan delta plots obtained by DMA at frequency of 1 Hz of the trays 6, 11, 13 and 14.

rate exceeds 50 °C min^{-1}. The conventional DSC equipment used in this study operates at lower heating rates, resulting in a very weak signal and hence no distinct step change in T_g transition was observed.[62]

DMA reveals the viscoelastic behaviour of materials under varying temperature conditions. It was employed to explore transitions such as glass transitions, and other thermal events, while also assessing the corresponding changes in mechanical properties. The plots of dynamic storage modulus E', and tan delta *versus* temperature for trays 6, 11, 13 and 14 are shown in Fig. 6a and b, respectively. The storage modulus decreases with increases in temperature (Fig. 6a). For the temperature of 25 °C, the storage modulus values are 436 MPa, 235 MPa, 160 MPa and 412 MPa for trays 6, 11, 13 and 14, respectively.

The divergence between the results obtained from three-point bending tests conducted on a conventional tensile machine that give lower flexural modulus for the tray 6 and single-point bending tests in a dynamic mechanical analyser (DMA) can be attributed to the different load transfer mechanisms associated with each method. One possible explanation is that the storage modulus measures the energy stored and recovered during elastic deformation, while the flexural modulus is related to the resistance of the trays to bending under an external load. Additionally, three-point bending provides a uniform stress distribution across the sample, whereas single-point bending creates a gradient of stress along the length of the sample. Although cellular materials are known for their ability to undergo loads without fracture, the high rigidity of the outer skin can inhibit effective load transfer. For rigid materials, as in this case, a concentrated force results in a high storage modulus, reflecting the material's ability to store and recover elastic energy efficiently. A parabolic pattern/profile was observed for Tan delta (Fig. 6b), with an indistinct T_g This can be due to various reasons, including structural heterogeneity, secondary relaxations, crystallinity effects, or compatibility in polymer blends. As the trays comprise 28% wt of primary paper sludge this broad hump indicates partial compatibility between the blend components, resulting in a wide range of dynamic relaxations.[63]

4 Conclusions

This study put in evidence the possibility of utilization of primary sludge from paper industry in the composition of

© 2025 The Author(s). Published by the Royal Society of Chemistry

Open Access Article. Published on 03 June 2025. Downloaded on 2/14/2026 7:58:34 PM. This article is licensed under a Creative Commons Attribution 3.0 Unported Licence.

starch-based foamed packaging materials obtained by extrusion-injection moulding. Therefore, this can be seen as a potential use of primary sludge for value-added application, as an alternative to landfill disposal. In this study, up to 28 wt% of primary sludge was introduced into the starch composites, a significant improvement compared to previous studies involving the addition of different biomass to starch composites, which typically reached up to 10 wt%. The produced trays packages demonstrated a cellular foamed structure featuring an outer hornified hard skin with hydrophobic nature highlighting the potential to be applied in packaging. At the same time, the foamed interior provides a relatively light material (dr of *ca.* 0.5) with high water absorption capacity. This fact is important from the point of view of the biodegradation potential and recycling. The small variations in the injection moulding parameters resulted in minor differences in the structural, mechanical resistance and tolerance to moist environments. Overall, this study demonstrated the possibility of production environmentally friendly 3D packaging materials from natural and waste materials using injection moulding, diverging from previous research trends that mainly used compression moulding for flat starch-based biocomposites.

Data availability

The data that supports the findings of this work are available within the article and in the ESI.†

Author contributions

SCP: writing – original draft, writing – review & editing. Methodology, investigation, formal analysis, conceptualization. BG: methodology, investigation, formal analysis, conceptualization. VGL: resources, visualization, investigation, project administration. DVE: writing – review & editing, validation, supervision, funding acquisition, conceptualization.

Conflicts of interest

There are no conflicts to declare.

Acknowledgements

This study was funded by the PRR – Recovery and Resilience Plan and by the Next GenerationEU funds at University of Aveiro, through the scope of the Agenda for Business Innovation "Transform – Transformação digital do setor florestal para uma economia resiliente e hipocarbónica" (project no. 34 with the application C644865735-00000007). This work was developed within the scope of the project CICECO-Aveiro Institute of Materials, UIDB/50011/2020 (**https://doi.org/10.54499/UIDB/50011/2020**), UIDP/50011/2020 (**https://doi.org/10.54499/UIDP/50011/2020**) & LA/P/0006/2020 (**https://doi.org/10.54499/LA/P/0006/2020**) and CEF, **https://doi.org/10.54499/UIDB/00239/2020**, both Centres financed by national funds through the FCT/MCTES (PIDDAC).

References

1 D. Costa, P. Quinteiro, V. Pereira and A. C. Dias, Social life cycle assessment based on input-output analysis of the Portuguese pulp and paper sector, *J. Clean. Prod.*, 2022, **330**, 129851.
2 T. Turner, R. Wheeler and I. W. Oliver, Evaluating land application of pulp and paper mill sludge: a review, *J. Environ. Manage.*, 2022, **317**, 115439.
3 M. Likon and P. Trebe in *Industrial Waste*, InTech, 2012.
4 A. Haile, G. G. Gelebo, T. Tesfaye, W. Mengie, M. A. Mebrate, A. Abuhay and D. Y. Limeneh, Pulp and paper mill wastes utilizations and prospects for high value-added biomaterials, *Bioresour. Bioprocess.*, 2021, **8**, 35.
5 P. Faubert, S. Barnabé, S. Bouchard, R. Côté and C. Villeneuve, Pulp and paper mill sludge management practices: what are the challenges to assess the impacts on greenhouse gas emissions?, *Resour. Conserv. Recycl.*, 2016, **108**, 107–133.
6 S. D. Ingale and P. D. Nemade, Effect of paper sludge ash on properties of cement concrete: a review, *Mater. Today Proc.*, 2023, DOI: **10.1016/j.matpr.2023.03.492**.
7 O. Kizinievič, V. Kizinievič, Y. Trambitski, R. Grubliauskas, O. Gencel, J. Malaiškienė and T. Astrauskas, Lightweight composite materials made of paper sludge and corn starch, *Ind. Crops Prod.*, 2024, **208**, 117847.
8 A. N. Grebenkin, E. L. Akim, A. A. Grebenkin, A. A. Pekarets and A. V. Demidov, Use of Fibrous and Mineral Pulp and Paper Wastes as Sorbents for Spilled Oil Products, *Fibre Chem.*, 2021, **53**, 82–87.
9 M. Hojamberdiev, Y. Kameshima, A. Nakajima, K. Okada and Z. Kadirova, Preparation and sorption properties of materials from paper sludge, *J. Hazard. Mater.*, 2008, **151**, 710–719.
10 J.-G. Rosenboom, R. Langer and G. Traverso, Bioplastics for a circular economy, *Nat. Rev. Mater.*, 2022, **7**, 117–137.
11 Y. Chen, A. K. Awasthi, F. Wei, Q. Tan and J. Li, Single-use plastics: production, usage, disposal, and adverse impacts, *Sci. Total Environ.*, 2021, **752**, 141772.
12 European Commission, *Energy, climate change, environment – single-use plastics*, **https://environment.ec.europa.eu/topics/plastics/single-use-plastics_en**, accessed, 6 February 2025.
13 A. Surendren, A. K. Mohanty, Q. Liu and M. Misra, A review of biodegradable thermoplastic starches, their blends and composites: recent developments and opportunities for single-use plastic packaging alternatives, *Green Chem.*, 2022, **24**, 8606–8636.
14 D. R. Tapia-Blácido, G. J. Aguilar, M. T. de Andrade, M. F. Rodrigues-Júnior and F. C. Guareschi-Martins, Trends and challenges of starch-based foams for use as food packaging and food container, *Trends Food Sci. Technol.*, 2022, **119**, 257–271.
15 A. J. F. Carvalho, in *Monomers, Polymers and Composites from Renewable Resources*, Elsevier, 2008, pp. 321–342.
16 S. V. G. Kumari, K. Pakshirajan and G. Pugazhenthi, Recent advances and future prospects of cellulose, starch, chitosan,

© 2025 The Author(s). Published by the Royal Society of Chemistry

Open Access Article. Published on 03 June 2025. Downloaded on 2/14/2026 7:58:34 PM. This article is licensed under a Creative Commons Attribution 3.0 Unported Licence.

polylactic acid and polyhydroxyalkanoates for sustainable food packaging applications, *Int. J. Biol. Macromol.*, 2022, **221**, 163–182.

17 M. Aldas, C. Pavon, J. López-Martínez and M. P. Arrieta, Pine Resin Derivatives as Sustainable Additives to Improve the Mechanical and Thermal Properties of Injected Moulded Thermoplastic Starch, *Appl. Sci.*, 2020, **10**, 2561.

18 D. K. M. Matsuda, A. E. S. Verceheze, G. M. Carvalho, F. Yamashita and S. Mali, Baked foams of cassava starch and organically modified nanoclays, *Ind. Crops Prod.*, 2013, **44**, 705–711.

19 H. M. C. Azeredo and K. W. Waldron, Crosslinking in polysaccharide and protein films and coatings for food contact – a review, *Trends Food Sci. Technol.*, 2016, **52**, 109–122.

20 L. do Val Siqueira, C. I. L. F. Arias, B. C. Maniglia and C. C. Tadini, Starch-based biodegradable plastics: methods of production, challenges and future perspectives, *Curr. Opin. Food Sci.*, 2021, **38**, 122–130.

21 Q. Duan, Z. Zhu, Y. Chen, H. Liu, M. Yang, L. Chen and L. Yu, Starch-Based Foams Nucleated and Reinforced by Polysaccharide-Based Crystals, *ACS Sustain. Chem. Eng.*, 2022, **10**, 2169–2179.

22 S. Kashyap and D. Datta, Process parameter optimization of plastic injection molding: a review, *Int. J. Plast. Technol.*, 2015, **19**, 1–18.

23 J. Castaño, R. Bouza, S. Rodríguez-Llamazares, C. Carrasco and R. V. B. Vinicius, Processing and characterization of starch-based materials from pehuen seeds (Araucaria araucana (Mol) K. Koch), *Carbohydr. Polym.*, 2012, **88**, 299–307.

24 E. Farotti and M. Natalini, Injection molding. Influence of process parameters on mechanical properties of polypropylene polymer. A first study, *Procedia Struct. Integr.*, 2018, **8**, 256–264.

25 A. I. Quilez-Molina, J. F. Le Meins, B. Charrier and M. Dumon, Starch-fibers composites, a study of all-polysaccharide foams from microwave foaming to biodegradation, *Carbohydr. Polym.*, 2024, **328**, 121743.

26 N. Soykeabkaew, C. Thanomsilp and O. Suwantong, A review: starch-based composite foams, *Composites, Part A*, 2015, **78**, 246–263.

27 N. M. Moo-Tun, G. Iñiguez-Covarrubias and A. Valadez-Gonzalez, Assessing the effect of PLA, cellulose microfibers and CaCO3 on the properties of starch-based foams using a factorial design, *Polym. Test.*, 2020, **86**, 106482.

28 B. G. Girija and R. R. N. Sailaja, Low-density polyethylene/plasticized tapioca starch blends with the low-density polyethylene functionalized with maleate ester: mechanical and thermal properties, *J. Appl. Polym. Sci.*, 2006, **101**, 1109–1120.

29 A. E. S. Vercelheze, F. M. Fakhouri, L. H. Dall'Antônia, A. Urbano, E. Y. Youssef, F. Yamashita and S. Mali, Properties of baked foams based on cassava starch, sugarcane bagasse fibers and montmorillonite, *Carbohydr. Polym.*, 2012, **87**, 1302–1310.

30 M. C. D. Dominic, D. dos Santos Rosa, P. H. Camani, A. S. Kumar, K. V. Neenu, P. M. S. Begum, D. Dinakaran, E. John, D. Baby, M. M. Thomas, J. M. Joy, J. Parameswaranpillai and M. R. Saeb, Thermoplastic starch nanocomposites using cellulose-rich Chrysopogon zizanioides nanofibers, *Int. J. Biol. Macromol.*, 2021, **191**, 572–583.

31 A. M. Ferreira, J. Martins, L. H. Carvalho and F. D. Magalhães, Biosourced Disposable Trays Made of Brewer's Spent Grain and Potato Starch, *Polymers*, 2019, **11**, 923.

32 J. Chen, X. Wang, Z. Long, S. Wang, J. Zhang and L. Wang, Preparation and performance of thermoplastic starch and microcrystalline cellulose for packaging composites: extrusion and hot pressing, *Int. J. Biol. Macromol.*, 2020, **165**, 2295–2302.

33 C. Chiarathanakrit, J. Mayakun, A. Prathep and K. Kaewtatip, Comparison of the effects of calcified green macroalga (Halimeda macroloba Decaisne) and commercial CaCO3 on the properties of composite starch foam trays, *Int. J. Biol. Macromol.*, 2019, **121**, 71–76.

34 International Organization for Standardization, *Paper, Board, Pulps and Cellulose Nanomaterials – Determination of Residue (Ash Content) on Ignition at 525 °C (ISO 1762:2019)*, 2019.

35 International Standard Organization, *Paper, Board, Pulps and Cellulosic Nanomaterials, Determination of Dry Matter Content by Oven-Drying Method Part 1: Materials in Solid Form (ISO 638-1:2022)*.

36 ASTM International, *Standard Test Methods for Water Vapor Transmission of Materials (ASTM E96)*, 2018.

37 G.-Y. Liou, C.-W. Su, P.-W. Huang, S.-J. Hwang, C.-T. Huang and H.-S. Peng, Fabrication and Property Characterization of Long-Glass-Fiber-Reinforced Polypropylene Composites Processed Using a Three-Barrel Injection Molding Machine, *Polymers*, 2022, **14**, 1251.

38 G. Tofani, J. de Nys, I. Cornet and S. Tavernier, Alternative Filler Recovery from Paper Waste Stream, *Waste Biomass Valorization*, 2021, **12**, 503–514.

39 J. P. Cruz-Tirado, R. Vejarano, D. R. Tapia-Blácido, G. Barraza-Jáuregui and R. Siche, Biodegradable foam tray based on starches isolated from different Peruvian species, *Int. J. Biol. Macromol.*, 2019, **125**, 800–807.

40 X. Wang, G. Zhao and G. Wang, Research on the reduction of sink mark and warpage of the molded part in rapid heat cycle molding process, *Mater. Des.*, 2013, **47**, 779–792.

41 H. Zhou, S. Zhang and Z. Wang, Multi-objective optimization of process parameters in plastic injection molding using a differential sensitivity fusion method, *Int. J. Adv. Des. Manuf. Technol.*, 2021, **114**, 423–449.

42 G.-Y. Liou, W.-J. Su, F.-J. Cheng, C.-H. Chang, R.-H. Tseng, S.-J. Hwang, H.-S. Peng and H.-Y. Chu, Optimize Injection-Molding Process Parameters and Build an Adaptive Process Control System Based on Nozzle Pressure Profile and Clamping Force, *Polymers*, 2023, **15**, 610.

43 C. Herniou-Julien, J. R. Mendieta and T. J. Gutiérrez, Characterization of biodegradable/non-compostable films

© 2025 The Author(s). Published by the Royal Society of Chemistry

Open Access Article. Published on 03 June 2025. Downloaded on 2/14/2026 7:58:34 PM. This article is licensed under a Creative Commons Attribution 3.0 Unported Licence.

made from cellulose acetate/corn starch blends processed under reactive extrusion conditions, *Food Hydrocoll.*, 2019, **89**, 67–79.

44 T. Hong, J.-Y. Yin, S.-P. Nie and M.-Y. Xie, Applications of infrared spectroscopy in polysaccharide structural analysis: progress, challenge and perspective, *Food Chem.: X*, 2021, **12**, 100168.

45 H. Lu, R. Ma, R. Chang and Y. Tian, Evaluation of starch retrogradation by infrared spectroscopy, *Food Hydrocoll.*, 2021, **120**, 106975.

46 C. Pozo, S. Rodríguez-Llamazares, R. Bouza, L. Barral, J. Castaño, N. Müller and I. Restrepo, Study of the structural order of native starch granules using combined FTIR and XRD analysis, *J. Polym. Res.*, 2018, **25**, 266.

47 J. Xiong, Q. Li, Z. Shi and J. Ye, Interactions between wheat starch and cellulose derivatives in short-term retrogradation: rheology and FTIR study, *Food Res. Int.*, 2017, **100**, 858–863.

48 S. Y. Oh, D. I. Yoo, Y. Shin, H. C. Kim, H. Y. Kim, Y. S. Chung, W. H. Park and J. H. Youk, Crystalline structure analysis of cellulose treated with sodium hydroxide and carbon dioxide by means of X-ray diffraction and FTIR spectroscopy, *Carbohydr. Res.*, 2005, **340**, 2376–2391.

49 D. Domene-López, J. C. García-Quesada, I. Martin-Gullon and M. G. Montalbán, Influence of Starch Composition and Molecular Weight on Physicochemical Properties of Biodegradable Films, *Polymers*, 2019, **11**, 1084.

50 J. J. G. van Soest, S. H. D. Hulleman, D. de Wit and J. F. G. Vliegenthart, Crystallinity in starch bioplastics, *Ind. Crops Prod.*, 1996, **5**, 11–22.

51 K. Dome, E. Podgorbunskikh, A. Bychkov and O. Lomovsky, Changes in the Crystallinity Degree of Starch Having Different Types of Crystal Structure after Mechanical Pretreatment, *Polymers*, 2020, **12**, 641.

52 L. Meng, H. Liu, L. Yu, Q. Duan, L. Chen, F. Liu, Z. Shao, K. Shi and X. Lin, How water acting as both blowing agent and plasticizer affect on starch-based foam, *Ind. Crops Prod.*, 2019, **134**, 43–49.

53 G. V. Laivins and A. M. Scallan, in *Trans. of the Xth Fund. Res. Symp. Oxford*, ed. C. F. Baker, Fundamental Research Committee (FRC), Manchester, 1993, pp. 1235–1260.

54 I. Portugal, V. M. Dias, R. F. Duarte and D. V. Evtuguin, Hydration of Cellulose/Silica Hybrids Assessed by Sorption Isotherms, *J. Phys. Chem. B*, 2010, **114**, 4047–4055.

55 J. Li, M. Zhou, G. Cheng, F. Cheng, Y. Lin and P.-X. Zhu, Fabrication and characterization of starch-based nanocomposites reinforced with montmorillonite and cellulose nanofibers, *Carbohydr. Polym.*, 2019, **210**, 429–436.

56 M. M. Hassan and I. J. Fowler, Thermal, mechanical, and rheological properties of micro-fibrillated cellulose-reinforced starch foams crosslinked with polysiloxane-based cross-linking agents, *Int. J. Biol. Macromol.*, 2022, **205**, 55–65.

57 H. Gonon, A. Srisa, K. Promhuad, V. Chonhenchob, N. Bumbudsanpharoke, L. Jarupan and N. Harnkarnsujarit, PLA thermoformed trays incorporated with cinnamaldehyde and carvacrol as active biodegradable bakery packaging, *Food Packag. Shelf Life*, 2023, **38**, 101123.

58 P. R. Salgado, V. C. Schmidt, S. E. M. Ortiz, A. N. Mauri and J. B. Laurindo, Biodegradable foams based on cassava starch, sunflower proteins and cellulose fibers obtained by a baking process, *J. Food Eng.*, 2008, **85**, 435–443.

59 H. Peidayesh, K. Mosnáčková, Z. Špitalský, A. Heydari, A. O. Šišková and I. Chodák, Thermoplastic Starch–Based Composite Reinforced by Conductive Filler Networks: Physical Properties and Electrical Conductivity Changes during Cyclic Deformation, *Polymers*, 2021, **13**, 3819.

60 E. Aguirre, J. Domínguez, E. Villanueva, J. A. Ponce-Ramirez, M. de Fátima Arevalo-Oliva, R. Siche, J. González-Cabeza and G. Rodríguez, Biodegradable trays based on Manihot esculenta Crantz starch and Zea mays husk flour, *Food Packag. Shelf Life*, 2023, **38**, 101129.

61 N. Calace, A. Di Muro, E. Nardi, B. M. Petronio and M. Pietroletti, Adsorption Isotherms for Describing Heavy-Metal Retention in Paper Mill Sludges, *Ind. Eng. Chem. Res.*, 2002, **41**, 5491–5497.

62 P. Liu, L. Yu, H. Liu, L. Chen and L. Li, Glass transition temperature of starch studied by a high-speed DSC, *Carbohydr. Polym.*, 2009, **77**, 250–253.

63 O. Fričová, M. Hutníková and H. Peidayesh, DMA study of thermoplastic starch/montmorillonite nanocomposites, *AIP Conf. Proc.*, 2021, 050004.

© 2025 The Author(s). Published by the Royal Society of Chemistry